NASA Contractor Report 3904

Ultrasonic Testing of Plates Containing Edge Cracks

James H. Williams, Jr., Hira Karagulle,
and Samson S. Lee

GRANT NAG3-328
JUNE 1985

NASA

NASA Contractor Report 3904

Ultrasonic Testing of Plates Containing Edge Cracks

James H. Williams, Jr., Hira Karagulle, and Samson S. Lee

Massachusetts Institute of Technology
Cambridge, Massachusetts

Prepared for
Lewis Research Center
under Grant NAG3-328

National Aeronautics
and Space Administration

Scientific and Technical Information Branch

1985

1. INTRODUCTION

Conventional ultrasonic testing (UT) techniques for the nondestructive evaluation (NDE) of macrostructural defect states of materials is generally divided into two categories; namely, the pulse- echo and through- transmission techniques [1]. In the pulse- echo technique, the transmitting and receiving transducers, which may be combined into a single transducer, are coupled to the same face of the test structure and the reflected wave field (echo) from the defect is analyzed in the time domain [1] or in the frequency domain [2]. The echo from a defect is affected by the defect type, shape, size and orientation, and diffraction of the incident ultrasonic wave. The received signal gives an accurate measure of the defect size only in a limited number of cases. Information on the defect has to be obtained through interpretation of the signals received at a variety of receiving transducer positions [3].

In the through- transmission technique, the transmitting and receiving transducers are coupled to the opposite faces of the test structure and the transmitted wave field is analyzed. Although the through- transmission technique is less subject to errors due to defect orientation and scattering, it still suffers from deficiencies such as defect transparancy [3].

For the characterization of cracks perpendicular to the faces of a test structure, special separate transmitting and receiving transducers with an inclined beam angle may be used and the principles of conventional pulse- echo or through- transmission techniques may be applied. These techniques are referred to as tandem or pitch- and- catch technique [1,3,4].

In another technique for the characterization of such cracks, the time delays of the diffracted waves from the edges of the crack may be used [5]. If

the crack is opened to the surface (surface- breaking crack) and access to that surface is available, Rayleigh waves may also be utilized to characterize the crack [3,6,7].

All the above techniques are limited to the analysis of nonoverlapping signals. Recently Vary et al. [8,9] introduced an ultrasonic NDE parameter called the "stress wave factor" (SWF). Separate transmitting and receiving transducers are coupled to the same face of the test structure, which is called the SWF configuration. An input pulse having a broadband frequency spectrum is applied to the transmitting transducer and the number of oscillations (or some modifications thereof [10]) in the output signal at the receiving transducer exceeding a preselected voltage threshold is defined as the SWF. The SWF is also valid for the analysis of the output signals with overlapping echoes.

The SWF analysis has shown encouraging results in several NDE applications [8- 11], and its use in new applications is currently under study [11].

The stress wave transmission characteristics of an isotropic elastic plate through which the transmitting and receiving transducers communicate in the SWF configuration are studied in [12] and [13]. The analysis of SWF output signals in the frequency domain is given in [14]. From the analyses in [12-14], the following can be stated for the SWF signal.

1. The SWF signal is the superposition of signals due to stress wave fields which multiply reflect between the top and bottom faces of the structure, simply reflections. Each reflection comes from a different direction and travels a different total ray path length. Reflections may be observed separately if the plate is sufficiently thick, or

they may overlap.

2. More advanced signal processing techniques [14] are needed for the analysis of the output, especially if the reflections are overlapped. However, more information can be obtained by analyzing only one output.
3. The output contains information about a larger volume of the plate as compared with the conventional techniques, and there is flexibility in specifying the testing region via changing the distance between the transmitting and receiving transducers.
4. The output is affected by the wave transmission properties of the plate in the direction parallel to its faces, the direction in which plates are loaded in many structures.
5. UT by utilizing the SWF configuration does not require access to both sides of the test structure.
6. If the thickness of the structure is less than the near field distance [12, 13] (which depends on the transmitting transducer radius and the signal wavelength) the measurements in the conventional pulse- echo and through- transmission techniques must be made in the near field, or the transmitting transducer and the plate may have to be located apart from each other in a fluid tank. However, in the SWF configuartion it may be possible to get information in the far field although the plate is thin, because there may be multiple reflections which travel a total ray path length greater than the far field distance [13]. The measurements in the far field are outside the interference region and, therefore, may be interpreted more easily.

The SWF has been generally used to characterize microstructural defect state of materials [8- 11]. In this study the experimental SWF output signals generated in plates containing cracks perpendicular to its faces are analyzed using the signal processing techniques discussed in [14]. The effects of the existence, lateral location and depth of the crack on the output signal characteristics are studied in the frequency domain.

2. EXPERIMENTS

The experimental system used in this study is characterized in [15] by coupling the transmitting and receiving transducers face- to- face, without a test specimen in between. The experimental system behaves as a linear- phase bandpass filter in the frequency range 0.6 to 2.3 MHz.

A schematic of the SWF configuration showing the experimental geometry is given in Fig. 1. The plate has a thickness h and its sides are far from the transducers so that reflections from the sides do not occur during the period of observation. The transducers have a radius a and are located on the top face of the plate at a distance ℓ apart. The crack has a depth d which is perpendicular to the plate faces. It is open to the bottom face of the plate throughout the depth (into the plane of the sketch) of the plate. It is located at a distance ℓ_c from the middle axis between the transducers, where ℓ_c is positive if the crack is located on the receiving transducer side of the middle axis as in Fig. 1.

The plates (25 cm x 25 cm x h) used in the experiments are made of 6061-T6 aluminum with longitudinal (P) and shear (S) wave velocities of 0.632 and 0.313 cm/μsec, respectively. The thicknesses of the plates and the depths of the cracks considered are listed in Table 1. All the cracks have a width of 0.05 cm. The codes assigned for specimens and some dimensionless quantities associated with the geometry of specimens and the P wavelengths λ_1 corresponding to several frequencies f are also given in Table 1.

The transducers (Panametrics model V105) have a radius a of 1.125 cm, and the distance between the transducer axes ℓ is 6 cm in all experiments. For specimens with nonzero crack depth, the location of the crack ℓ_c is changed

from -4 to 4 cm with in increments of 0.5 cm.

The time history of the input signal is shown in Fig. 2. It has a -6 dB frequency band of 0.4 to 3 MHz. The signal in Fig. 2 and all the time domain signals in the subsequent figures are discrete; their sampling period being 0.05 μsec (sampling frequency 20 MHz). The discrete points are connected by linear interpolation.

The input signal in Fig. 2 is the same in all experiments except for specimens with h=10 cm (C0, C1, C2). For specimens with h=10 cm the input has the same waveform but scaled by approximately 0.3 compared with the input signal in Fig. 2.

3. PROCESSING OF SWF OUTPUT SIGNALS

Typical SWF output signals for some cases are shown in Figs. 3- 5. As in [13], the reflection which is generated by the stress wave fields which travel p times as a P wave and s times as an S wave through the plate while reflecting back and forth between the bottom and top faces of the plate is designated as the reflection with p,s. The time delays for some possible reflections are calculated using the formulae given in [12] and [13], which are derived by considering the multiply reflected rays constructed geometrically according to Snell's law; these are indicated above the output signals in Figs. 3, 4 and 5 with the values of p and s.

As observed from Fig. 3, the reflections in the output signals for specimens A0 and A1 (with h=2.4 cm) are not overlapped significantly. This nonoverlapping case exists because the thickness of the plate is sufficiently large that the difference between the time delays for the successive significant reflections is adequately large. On the other hand, the reflections in the output signals for specimens B0 and B1 (with h=1.25 cm) are overlapped as observed from Fig. 4. Also, the output signals shown in Fig.5 for specimens C0 and C2 (with h=10 cm) contain nonoverlapping reflections.

The digital signal processing techniques applied to SWF signals to obtain information in the frequency domain on individual reflections are discussed in [14]. Short- time portions of the SWF signals are considered. If significant reflections in a SWF signal are not overlapped, the short- time Fourier analysis is used. The data window, which defines the short- time SWF signal, includes only an individual reflection and completely excludes all the other reflections. Then, by calculating the fast Fourier transform (FFT) of

the short- time SWF signal, the magnitude spectrum of the individual reflection is found directly.

If reflections in a SWF signal are overlapped, the short- time homomorphic analysis, which is also called the short- time cepstrum analysis, is used. The inverse fast Fourier transform (IFFT) of the logarithmic magnitude spectrum (log spectrum) of a time domain signal is called the cepstrum. The cepstrum is again a time domain signal and is symmetric about zero. In order to find an estimate of the magnitude spectrum of an individual reflection, the cepstrum of the short- time SWF signal is multiplied by a cepstrum window which covers the low- time portion of the cepstrum. Then the FFT and exponentiation operations are applied to the windowed cepstrum, resulting in the estimate to the magnitude spectrum of the individual reflection. For the analysis to be valid, the data window and the cepstrum window must be specified appropriately, the conditions for which are discussed in [14] in detail.

The types of the methods of analysis and the specifications of the data windows for finding the magnitude spectra of some reflections with only P waves (s=0) are given in Table 2 for specimens A0, B0, C0 (with d=0). The reflections considered for each specimen are specified by the values of p. The ray angles, total ray path lengths, and time delays for the reflections are calculated using the formulae given in [12] and [13]. These are also indicated in Table 2. The cepstrum window used in the short- time homomorphic analysis is a Hamming window with an interval of -1.25 to 1.25 μsec.

For any other specimen having the same plate thickness as any of the specimen A0 or B0 or C0 the corresponding same conditions given in Table 2 are considered.

4. RESULTS AND DISCUSSIONS

The characteristics of a log spectrum such as the peak frequency f_p; lower and upper frequencies of -3 dB frequency band f_1 and f_2, respectively; lower and upper frequencies of -6 dB frequency band f_3 and f_4, respectively; average resonant frequency f_c; peak log magnitude Y_p; log magnitude at average resonant frequency Y_c; and average log magnitude over - 3 dB frequency band (simply the average log magnitude) Y_a are defined in Fig. 6 on a hypothetical log spectrum.

The values of the average log magnitude and the average resonant frequency for a particular reflection in a specimen without a crack are denoted by $[Y_a]_o$ and $[f_c]_o$;'respectively; and these are listed in Table 3 for different reflections in specimens A0, B0, and C0. The statistical behaviors of $[Y_a]_o$ and $[f_c]o$ which are evaluated from three sets of repeated experiments, each are also given in Table 3. Notice that the frequencies considered in Table 1 cover the range of frequencies that appears in Table 3.

How the existence, lateral location, and depth of the cracks in specimens with h=2.4 cm (A0, A1, A2, and A3) affect the average log magnitude Y_a of the log spectra of the reflections considered is studied in Fig. 7. Figs. 7 (a), 7 (b), and 7 (c) show the behavior of $Y_a-[Y_a]_o$ for the reflections with p=8, 10, and 12, respectively, versus ℓ_c for different d. The locations of the transducers and the middle axis are indicated in the figures. The data points at the beginning and the end of the abscissa (location of crack axis) in the figures correspond to the specimen without crack (A0). They are generated from separate experiments "under identical experimental" conditions. For the data point at the beginning of the abscissa, $Y_a-[Y_a]_o$ is

exactly zero. For the data point at the end of the abscissa, $Y_a - [Y_a]_o$ is approximately zero.

If there were no crack in the specimens with h=2.4 cm then all of the specimens would be identical and $Y_a - [Y_a]_o$ would be approximately zero within a threshold value for all the data points in Figs. 7 (a), 7(b) and 7 (c). The value of the threshold limit depends on the repeatibility of the experiments "under identical experimental" conditions. This value can be estimated using the standard deviation values for $[Y_a]_o$ given in Table 3. Thus, the changes in $Y_a - [Y_a]_o$ above the threshold limit in Figs. 7 (a), 7(b) and 7 (c) are due to the the the existence of cracks.

There are several observations which can be made from Figs. 7 (a), 7 (b), and 7 (c).

1. The change in $Y_a - [Y_a]_o$ versus ℓ_c is approximately symmetric about the middle axis.
2. $Y_a - [Y_a]_o$ is negative if the crack is located between the transducer axes; that is, if $|\ell_c| < 3$ where $|\ \ |$ denotes the "magnitude of". On the other hand, $Y_a - [Y_a]_o$ "is generally positive" when $|\ell_c| > 3$.
3. The magnitude of the negative values of $Y_a - [Y_a]_o$ is increasing for increasing crack depth d in the region where $|\ell_c| \leq 2$. The average of the data points in the region with $|\ell_c| \leq 2$ for a particular reflection (p) and a particular crack depth (d) is called the average dB drop and it is denoted by $[Y_a]_m - [Y_a]_o$.

4. The average dB drop versus 100 d/h is shown in Fig. 7 (d) for the different reflections (with p=8, 10, and 12) considered in specimens with h=2.4 cm. It is observed that the average dB drop for a particular d/h is approximately the same for each reflection considered.

Fig. 8 shows how a particular reflection (with p=4, s=0) interacts with a crack. It is shown in [13] that a receiving point in the far field observes the stress wave field for a particular reflection as a plane wave propagating and multiply reflecting in the directions specified by the ray which is constructed geometrically between the receiving point and the center of the transmitting transducer using Snell's law for that particular reflection. Such a multiply reflected ray is constructed in Fig. 8 (a).

In order to observe the scattering effect of the crack more clearly, consider the hypothetical multi- layered half- space shown in Fig. 8 (b), which is introduced in [13]. It is assumed that the successive back and forth reflections at the bottom and top faces of the original plate take place as transmissions through the boundaries of layers. The layers are assumed to be bonded together in a hypothetical way such that an incident wave in one layer produces no reflected waves but produces transmitted waves in the next layer with the transmission coefficients that are the same as the reflection coefficients as if the incident wave reflects at a stress- free plane boundary. In this description, the top layer can be thought of as the original layer and each subsequent layer can be thought of as the image of the layer immediately above it. The ray corresponding to the multiply reflected ray in Fig. 8 (a) is depicted in Fig. 8 (b). Notice that the images of the crack also appear in the image layers in Fig. 8 (b).

The description in Fig. 8 (b) then suggests that a reflection with a particular value of p and s "sees" the (p+s)/2 cracks which are twice the size of the original crack. If the cracks are located between the transducer axes as in Fig. 8 (b), they direct some of the incident energy away from the receiving transducer, which may cause a drop in the energy of the waves arriving at the receiving transducer, as compared with the no- crack case. If the cracks are not located between or on the transducer axes, they direct some of the incident energy toward the receiving transducer; energy which would otherwise not reach the receiving transducer if there were no cracks. This may cause an increase in the energy of the waves arriving at the receiving transducer.

As the location of a crack changes, scattered field from the crack changes and thus the field observed at the receiving transducer changes. For the crack sizes, location of transducers and frequencies considered in plates with h=2.41 cm, these changes do not affect the condition that the larger the crack the larger the drop in $Y_a - [Y_a]_o$ observed in Figs. 7 (a), 7 (b), and 7 (c).

The reflections with larger p (s=0) are affected by the crack with larger times as discussed above. On the other hand, for increasing p the angle between the propagation direction and crack becomes smaller, which decreases effect of the crack on the wave. This explains qualitatively why all the reflections undergo approximately the same average dB drop for a particular d/h, as seen in Fig. 7 (d).

The analysis for specimens with h=2.4 cm in Fig. 7 is repeated for specimens with h=1.25 cm (B0, B1, B2, and B2) and with h=10 cm (C0, C1, and C2) in Figs. 9 and 10, respectively. The data for the average dB drop versus

100 d/h for different groups of specimens in Figs. 7 (d), 9(d), and 10 (d) are superposed in Fig. 11. The line which is fitted to the superposed data by using least- squares criterion [16] is also shown.

Each data point in Fig. 11 satisfies the following condition :

$$100\,\frac{d}{h} = -7\,\{[Y_a]_m - [Y_a]_o\} + \text{Error} \qquad (1)$$

where -7 is the slope of the correlation line in Fig. 11.

The error values in eqn. (1) for the data points in Fig. 11 are given in Table 4. The absolute value of the error is less than 10 in most cases, however it reaches a maximum value of 14.9.

How the existence, lateral location and depth of the cracks affect the peak log magnitudes Y_p and the log magnitudes at average resonant frequencies Y_c are also studied. The same results shown in Figs. 7 and Figs. 9- 11 are obtained, but they are not repeated here.

The effect of cracks on the average resonant frequencies f_c is studied for the same reflections considered for the specimens with h=2.4 cm. The results are shown in Fig. 12. Again, the change in $f_c - [f_c]_o$ versus ℓ_c is symmetric about the middle axis. Here the change in $f_c - [f_c]_o$ is larger if the crack is located near (either) one of the transducer axes. However, there is no simple interpretation in terms of correlating the change in $f_c - [f_c]_o$ to the crack depths.

Similar results are obtained for other groups of specimens with h=1.25 cm and h=10 cm. Again no simple correlation between $f_c - [f_c]_o$ and the crack depths are observed.

Similar results are also obtained for the peak frequencies f_p ; lower and

upper frequencies of -3 dB frequency band f_1 and f_2, respectively; and lower and upper frequencies of -6 dB frequency band f_3 and f_4, respectively. Again no simple correlation to the crack depths can be stated at this point. The effect of a crack on all these characteristics are under current investigation.

5. CONCLUSIONS AND RECOMMENDATIONS

The stress wave factor (SWF) signal, which is the output of an ultrasonic testing (UT) system where the transmitting and receiving transducers are coupled to the same face of the test structure, was analyzed for the nondestructive evaluation (NDE) of plates containing perpendicular edge cracks. The transducers were located at the top face of the plate. The crack was open to the bottom face throughout the depth of the plate.

The effects of the existence, lateral location and depth of the crack on the log spectra of individual reflections in the SWF signal were studied. If the reflections in the SWF signal were not overlapped, the short- time Fourier analysis was applied to obtain the log spectra of the individual reflections. If the reflections were overlapped, the short- time homomorphic analysis (cepstrum analysis) was applied.

Aluminum plates with thicknesses h=1.25, 2.4, and 10 cm were used. Cracks with 100 d/h= 25, 50, and 75 in plates with h=1.25 and 2.4 cm, where d was the crack depth, and cracks with 100 d/h= 6 and 12 in plates with h=10 cm were considered. The transducers which had a radius of 1.125 cm were located 6 cm apart.

Plates with h=1.25 cm contained overlapping reflections and plates with h=2.4 and 10 cm contained nonoverlapping reflections. The log spectra of several reflections which had average resonant frequencies approximately at 0.9, 1.3, and 1.7 MHz were analyzed. It was observed that the average log magnitudes of the log spectra decreased more with increasing d/h if the crack was located between the transducers. The average decrease in average log magnitudes for different crack locations between the transducers was called

the average dB drop.

It was observed that the average dB drop versus 100 d/h was approximately linear. Also, the linearity was approximately the same for each reflection and each group of plates with the different thicknesses considered. By using the least- squares criterion, the slope of the correlation line for all the data was found to be 1 dB per 0.07 d/h.

Changes in the average resonant frequencies of the log spectra were also observed due to the existence of a crack and to changes in the location of the crack. However, no simple correlation between the average resonant frequency and crack depth could be stated at this point.

This study provides a quantitative analysis of the effects of the existence, lateral location and depth of a perpendicular crack on the SWF signal in plates. The analysis should be extended for cracks with different orientations and shapes and for different frequency ranges. Scattering theories should also be utilized to develop more quantitative analyses.

REFERENCES

[1] J. Krautkramer and H. Krautkramer, Ultrasonic Testing of Materials, Second Edition, Springer- Verlag, N.Y., 1977.

[2] D.W. Fitting and L. Adler, Ultrasonic Spectral Analysis for Nondestructive Evaluation, Plenum Press, N.Y., 1981.

[3] A. Rogerson and R.A. Murgatroyd, "Defect Characterization Using Ultrasonic Techniques", Research Techniques in Nondestructive Testing, Vol. IV, Ed. by R.S. Sharpe, Academic Press, Inc., New York, N.Y., 1980, pp. 451- 507.

[4] A. de Sterke, "Some Aspects of Radiography and Ultrasonic Testing of Welds in Steel with Thicknesses from 100- 300 mm.", The British Journal of Nondestructive Testing, Vol.9, No. 4, December 1967, pp. 94- 107.

[5] M.G. Silk, "Defect Sizing Using Ultrasonic Diffraction", The British Journal of Nondestructive Testing, Vol. 21, No. 1, January 1979, pp. 12- 15.

[6] A. Klein and H.J. Salzburger, "Characterization of Surface Defects by Rayleigh- Waves", New Procedures in Nondestructive Testing, Ed. by P. Holler, Springer- Verlag, Berlin, West Germany, 1983, pp.193- 202.

[7] D.W. Fitting and L. Adler, "Frequency Dependent Interaction of

Ultrasonic Waves with Surface- Breaking Cracks", New Procedures in Nondestructive Testing, Ed. by P. Holler, Springer- Verlag, Berlin, West Germany, 1983, pp. 203- 212.

[8] A. Vary and R.F. Lark, "Correlation of Fiber Composite Tensile Strength with the Ultrasonic Stress Wave Factor", Journal of Testing and Evaluation, Vol. 7, No. 4, July 1979, pp. 185- 191.

[9] A. Vary and K.J. Bowles, "An Ultrasonic- Acoustic Technique for Nondestructive Evaluation of Fiber Composite Quality", Polymer Engineering and Science, Vol. 19, No. 5, April 1979, pp. 373- 376.

[10] J.H. Williams, Jr. and N.R. Lampert, "Ultrasonic Evaluation of Impact-Damaged Graphite- Fiber Composite", Materials Evaluation, Vol. 38, No. 12, December 1980, pp. 68- 72.

[11] R.H. Wehrenberg II, "New NDE Technique Finds Subtle Defects", Materials Engineering, Vol. 92, No. 3, September 1980, pp. 59- 63.

[12] J.H. Williams, Jr., H. Karagulle, and S.S. Lee, "Ultrasonic Input-Output for Transmitting and Receiving Longitudinal Transducers Coupled to Same Face of Isotropic Elastic Plate", Materials Evaluation, Vol. 40, No. 6, May 1982, pp. 655-662.

[13] H. Karagulle, J.H. Williams, Jr., and S.S. Lee, "Stress Waves in an Isotropic Elastic Plate Excited by a Circular Transducer", Composite

Materials and Nondestructive Evaluation Laboratory, Massachusetts Institute of Technology, Cambridge, Mass., Unpublished Report, 1984.

[14] H. Karagulle, J.H. Williams, Jr., and S.S. Lee, "Application of Homomorphic Signal Processing to Stress Wave Factor Analysis", Composite Materials and Nondestructive Evaluation Laboratory, Massachusetts Institute of Technology, Cambridge, Mass., Unpublished Report, 1985..

[15] H. Karagulle, S.S. Lee, and J.H. Williams, Jr., "Input- Output Characterization of an Ultrasonic Testing System by Digital Signal Analysis", Report no. CR-3756, National Aeronautics and Space Administration, Washington, D.C., January 1984.

[16] R.W. Hornbeck, Numerical Methods, Prentice- Hall, Inc., Englewood Cliffs, N.J., 1975.

TABLE 1 Geometrical Properties of Specimens and Some Associated Dimensionless Quantities.

Specimen Code	h (cm)	d (cm)	$\frac{d}{h}$	For f=0.9 MHz (λ_1=0.70 cm)		For f=1.3 MHz (λ_1=0.70 cm)		For f=1.7 MHz (λ_1=0.37 cm)	
				$\frac{h}{\lambda_1}$	$\frac{d}{\lambda_1}$	$\frac{h}{\lambda_1}$	$\frac{d}{\lambda_1}$	$\frac{h}{\lambda_1}$	$\frac{d}{\lambda_1}$
A0	2.4	0	0	3.4	0	4.9	0	6.5	0
A1		0.6	0.25		0.9		1.2		1.6
A2		1.2	0.50		1.7		2.4		3.2
A3		1.8	0.75		2.6		3.7		4.9
B0	1.25	0	0	1.8	0	2.6	0	3.4	0
B1		0.31	0.25		0.4		0.6		0.8
B2		0.62	0.50		0.9		1.2		1.7
B3		0.93	0.75		1.3		1.9		2.5
C0	10	0	0	14.3	0	20.4	0	27	0
C1		0.6	0.06		0.9		1.2		1.6
C2		1.2	0.12		1.7		2.4		3.2

TABLE 2 Methods of Analysis and Specifications of Data Windows to Find Magnitude Spectra of Reflections With Only P Waves; and Ray Angles, Total Ray Path Lengths, and Time Delays of Reflections in Some Specimens.

Specimen Code	Reflection (Value of p)	Data Window			Ray Angle (Degree)	Total Ray Path Length (cm)	Time Delay (μsec)
		Type	Interval (μsec)				
			From	To			
A0	8	STF[a]	31.8	35.3	17.35	20.12	31.83
	10		39.1	42.6	14.04	24.74	39.14
	12		46.5	50	11.77	29 42	46.55
B0	12	STH[b]	16.95	34.95	21.80	16.16	25.56
	18		28.45	46.45	14.93	23.29	36.85
	22		35.95	53.95	12.31	28.15	44.54
C0	2	STF[a]	31.5	39	16.70	20.88	33.04
	4		62	69.5	8.53	40.45	64.00
	6		93	100.5	5.71	60.30	95.41

a STF : Short-time Fourier analysis (512-point FFT is used.)
b STH : Short-time homomorphic analysis (512-point FFT and IFFT are used in the process. The cepstrum window used in the process is a Hamming window having a duration from -1.25 to 1.25 μsec.)

TABLE 3 Values of f_o and $M_o(f_o)$ for Some Reflections in Specimens Without Crack and their Statistical Behaviors.

Specimen	Reflection (Value of p)	f_o (MHz)	$\tilde{M}_o(f_o)$ (dB)	Mean Value of f_o (MHz)	Standard Deviation in f_o (MHz)	Mean Value of $\tilde{M}_o(f_o)$ (dB)	Standard Deviation in $\tilde{M}_o(f_o)$ (dB)
A0	8	1	8.32	0.95	0.034	8.54	0.18
	10	1.19	9.33	1.16	0.018	9.87	0.39
	12	1.49	7.38	1.47	0.015	8.23	0.62
B0	12	0.97	-1.13	0.96	0.010	-1.24	0.85
	18	1.38	-2.14	1.37	0.014	-2.03	0.16
	22	1.41	-4.38	1.40	0.018	-4.38	0.35
C0	2	0.88	6.64	0.86	0.014	6.68	0.04
	4	1.37	16.09	1.36	0.006	16.07	0.08
	6	1.68	14.01	1.65	0.021	14.33	0.26

TABLE 4 Values of Error in Eqn. (1) for Data Points in Fig. 11.

Group of Specimens	$\frac{d}{h}$	Reflection (Value of p)	Value of Error in Eqn. (1) (percent)
A0, A1, A2, A3	0.25	8	-0.6
		10	-7.1
		12	-7.5
	0.50	8	-6.3
		10	-6.3
		12	-11.8
	0.75	8	4.4
		10	14.6
		12	5.7
B0, B1, B2, B3	0.25	12	-5.4
		18	0.4
		22	3.1
	0.50	12	-6
		18	5
		22	14.9
	0.75	12	-3.2
		18	-6.8
		22	-4.1
C0, C1, C2	0.06	2	0.4
		4	4.8
		6	1.7
	0.12	2	2.6
		4	7.3
		6	3.6

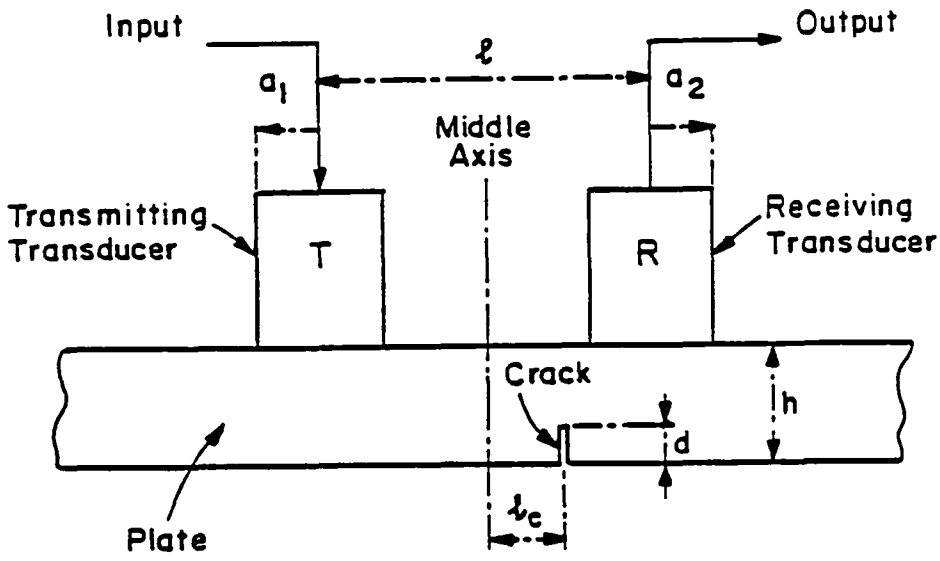

Fig. 1 Schematic of ultrasonic (stress wave factor) configuration showing geometry of plate, crack, and locations of transducers.

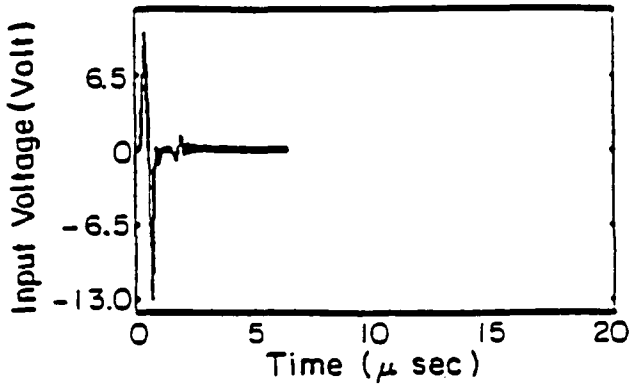

Fig. 2 Time history of input signal.

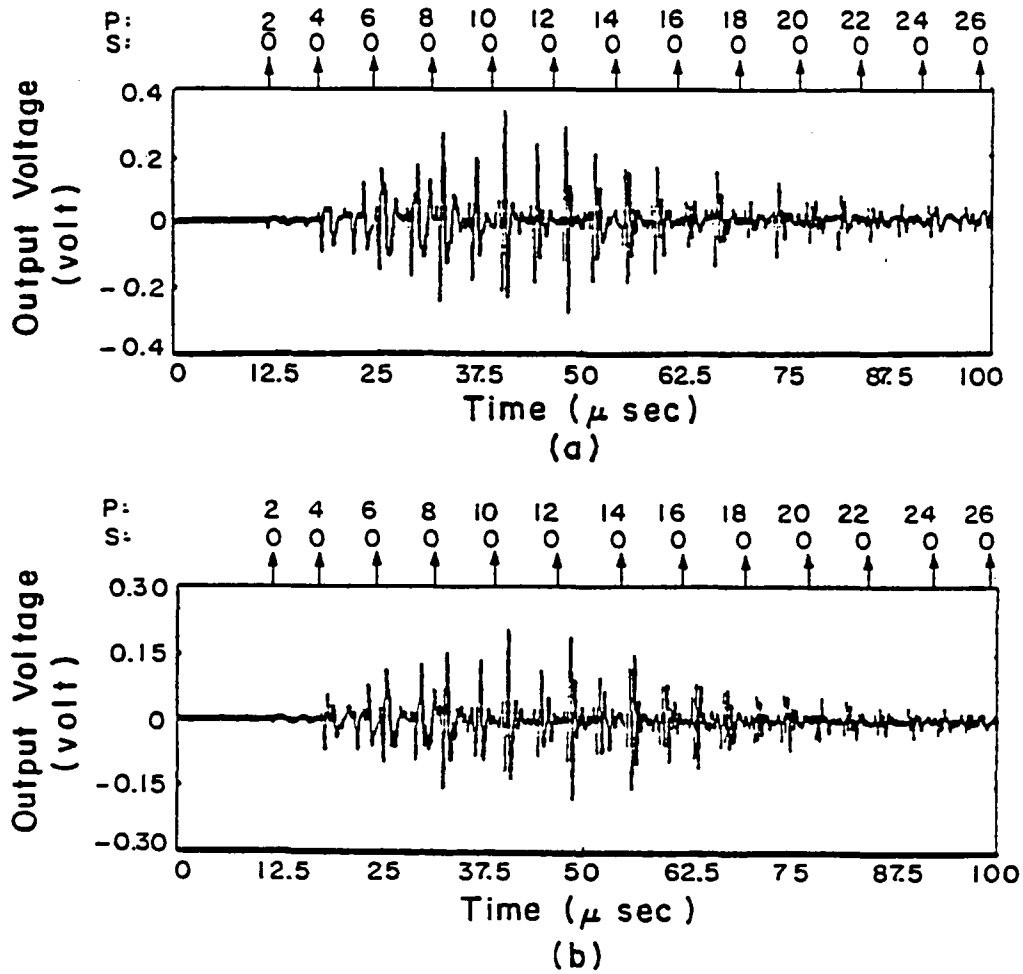

Fig. 3 Time histories of output signals for specimens with $\ell_c = 0$ for (a) A0 (h=2.4 cm, d=0), and (b) A1 (h=2.4 cm, d=0.6 cm).

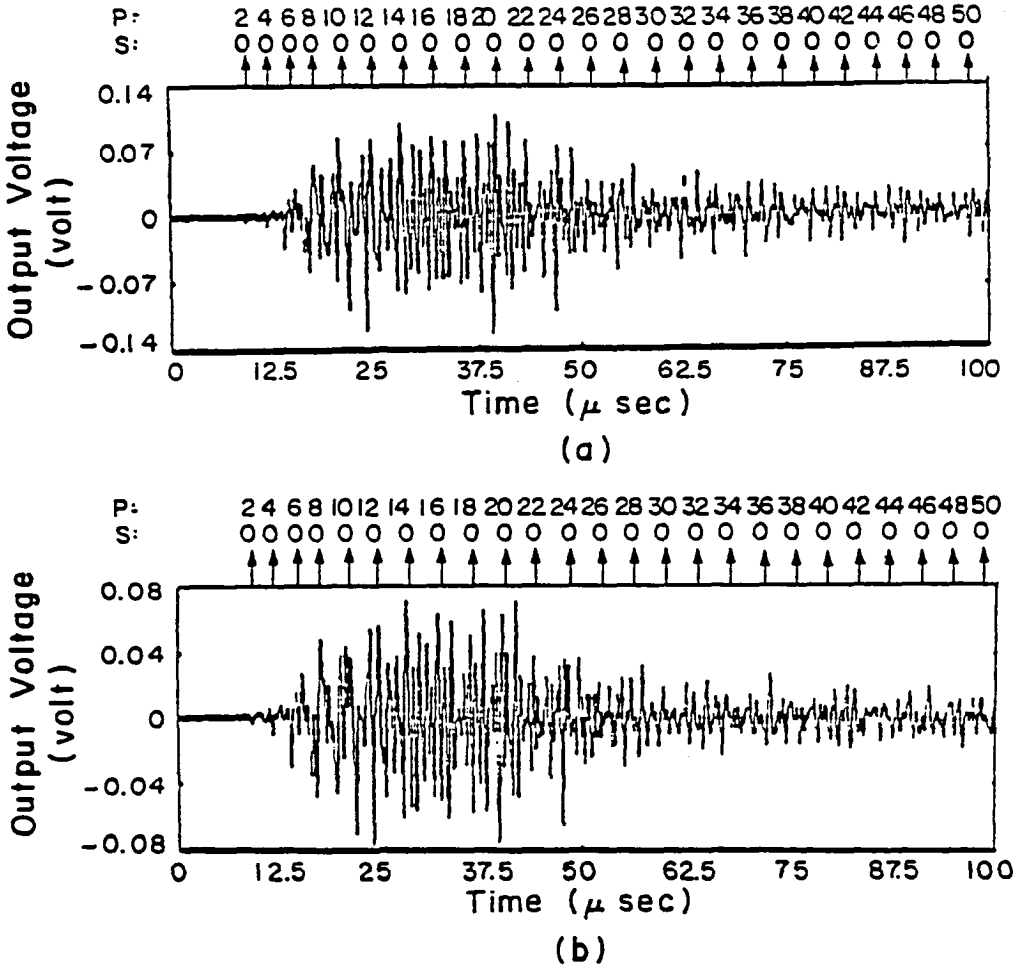

Fig. 4 Time histories of output signals for specimens with ℓ_c=0 for (a) B0 (h=1.25 cm, d=0), and (b) B1 (h=1.25 cm, d=0.31 cm).

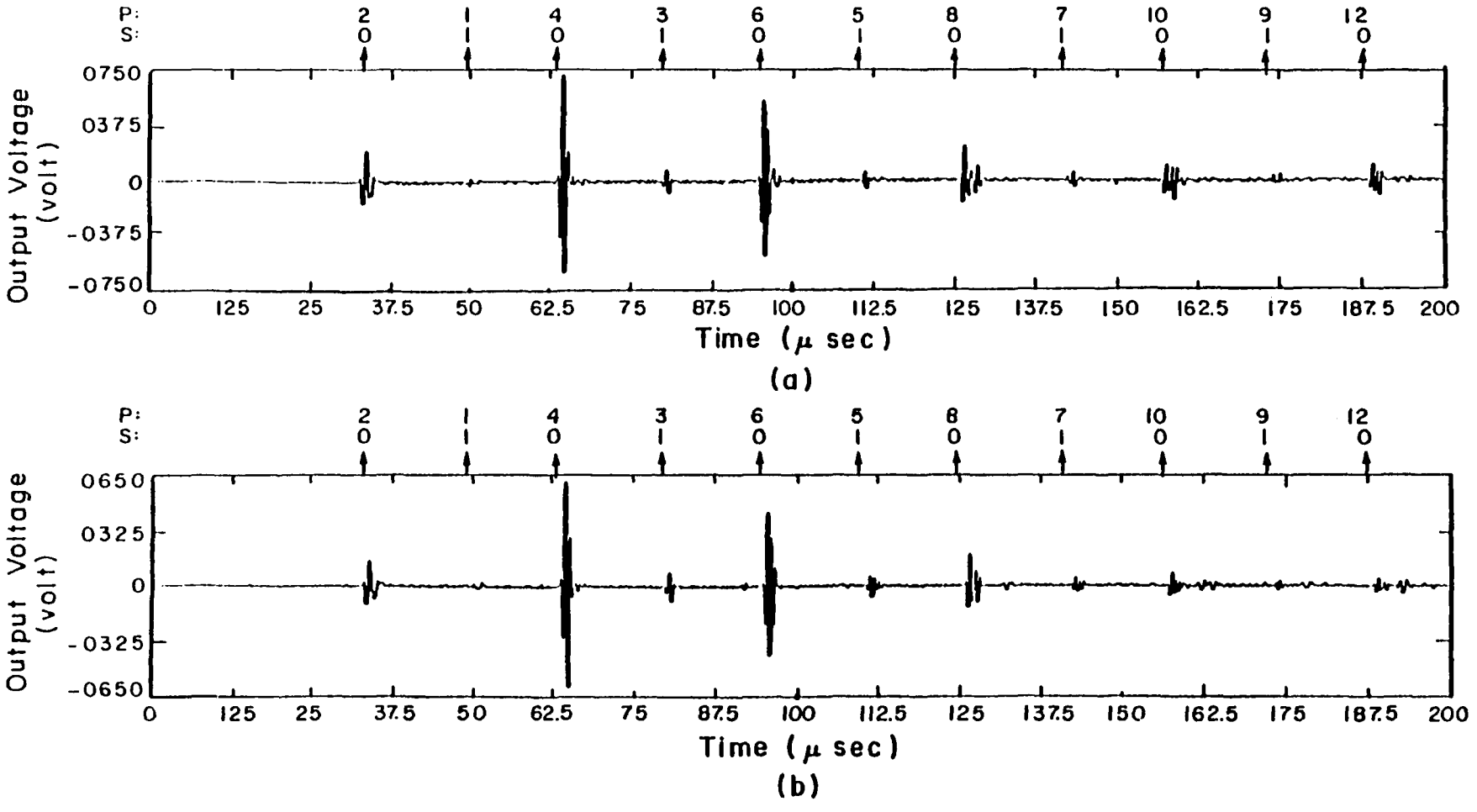

Fig. 5 Time histories of output signals for specimens with ℓ_c for (a) C0 (h=10 cm, d=0), and (b) C2 (h=10 cm, d=1.2 cm).

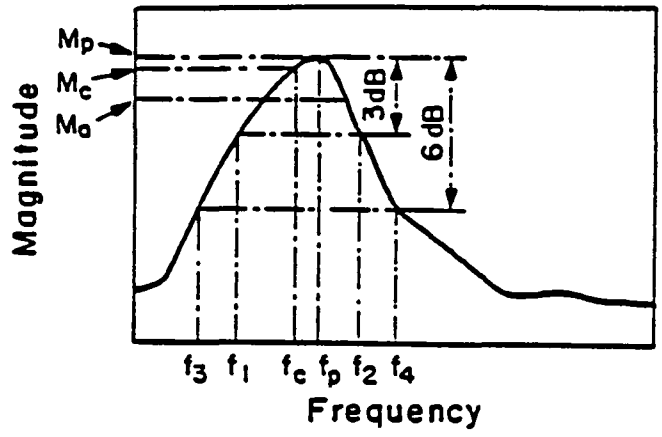

f_p	: Peak frequency
f_1	: Lower frequency of -3 dB frequency band
f_2	: Upper frequency of -3 dB frequency band
f_3	: Lower frequency of -6 dB frequency band
f_4	: Upper frequency of -6 dB frequency band
$f_c=(f_1+f_2)/2$	: Average resonant frequency
M_p	: Peak magnitude
M_c	: Magnitude at average resonant frequency
M_a	: Average magnitude over -3 dB frequency band

Fig. 6 Definitions of parameters on hypothetical magnitude spectrum.

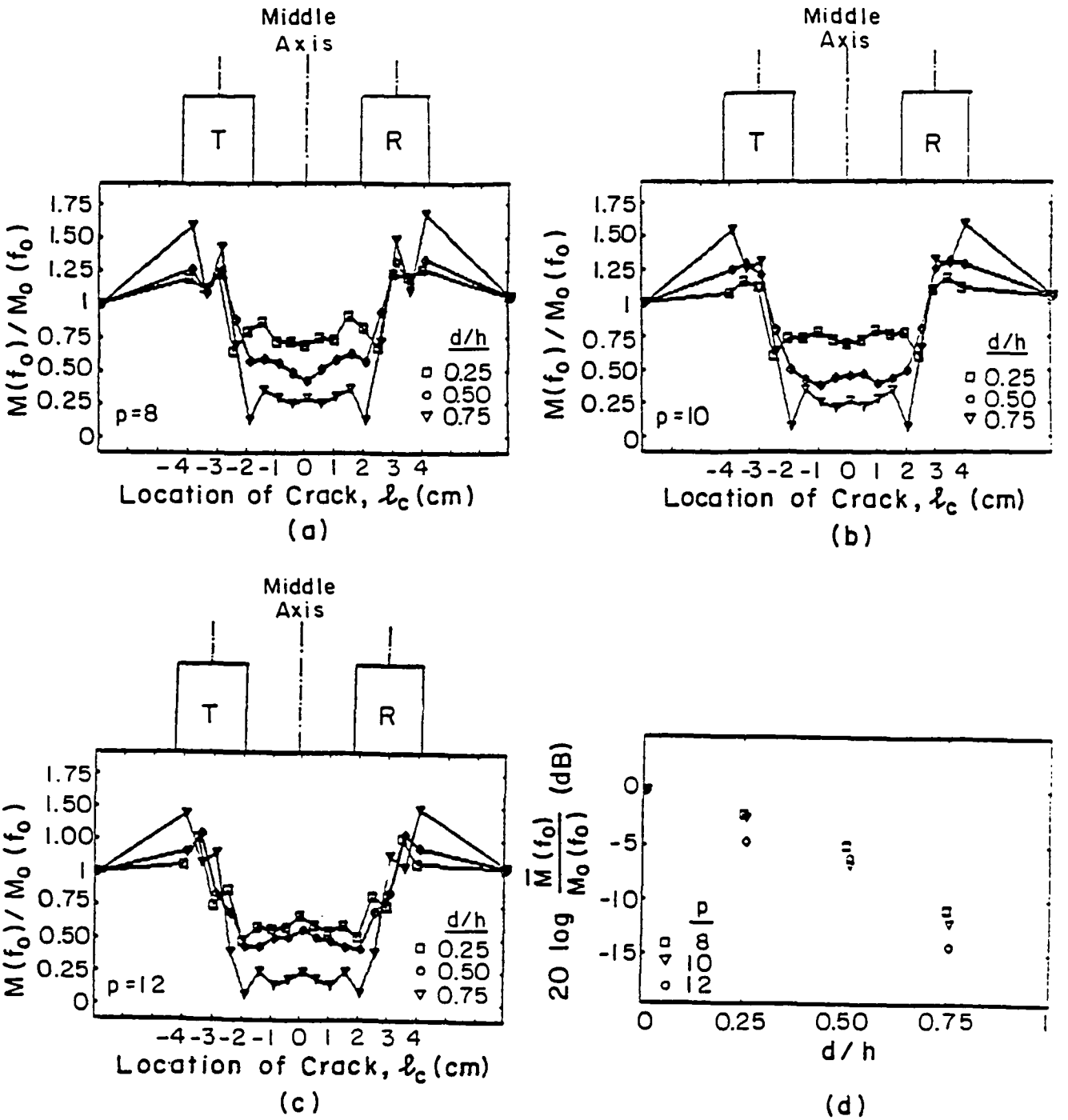

Fig. 7 $M(f_o)/M_o(f_o)$ for reflections with (a) p=8, (b) p=10, and (c) p=12 versus ℓ_c for different d; and (d) 20 Log$[M(f_o)/M_o(f_o)]$ versus d/h for different p in specimens with h=2.4 cm (A0, A1, A2, and A3).

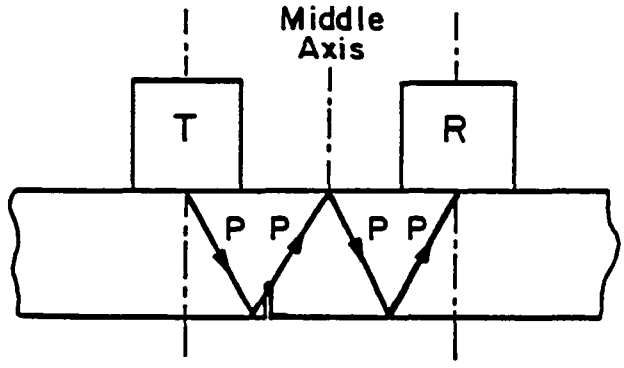

(a)

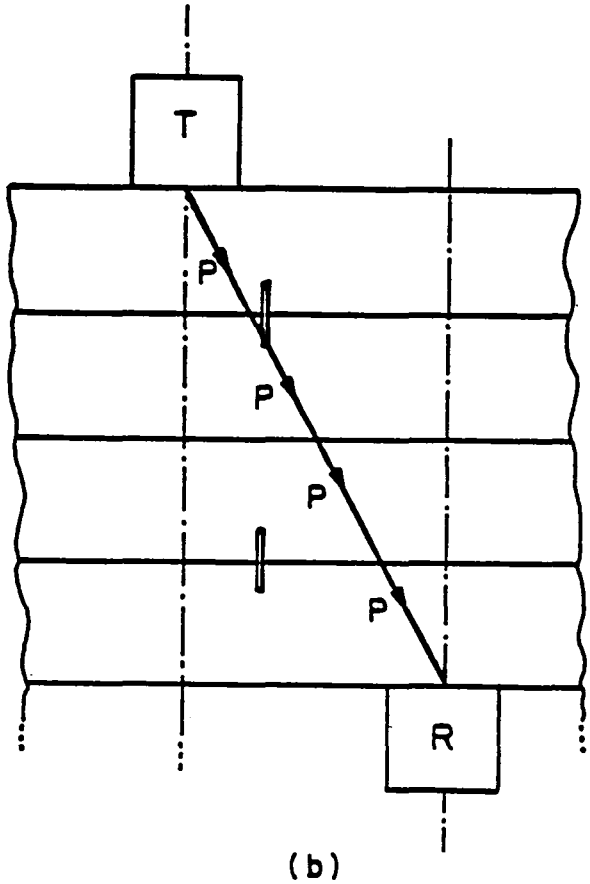

(b)

Fig. 8 (a) Plate with crack and the ray for the reflection with p=4, s=0 ; and (b) hypothetical multi-layered medium description.

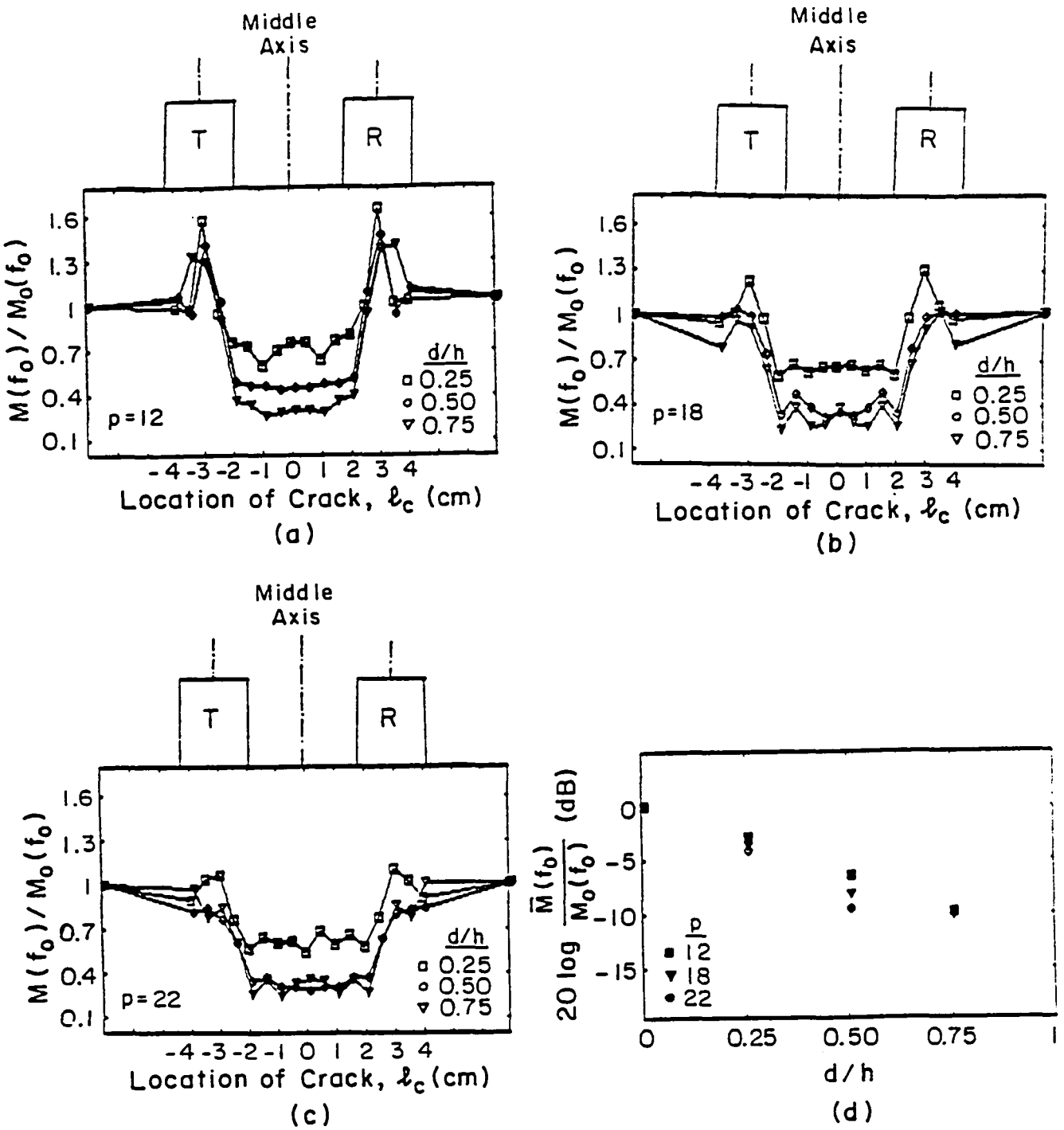

Fig. 9 $M(f_o)/M_o(f_o)$ for reflections with (a) p=12, (b) p=18, and (c) p=22 versus ℓ_c for different d; and (d) 20 Log$[M(f_o)/M_o(f_o)]$ versus d/h for different p in specimens with h=1.25 cm (B0, B1, B2, and B3).

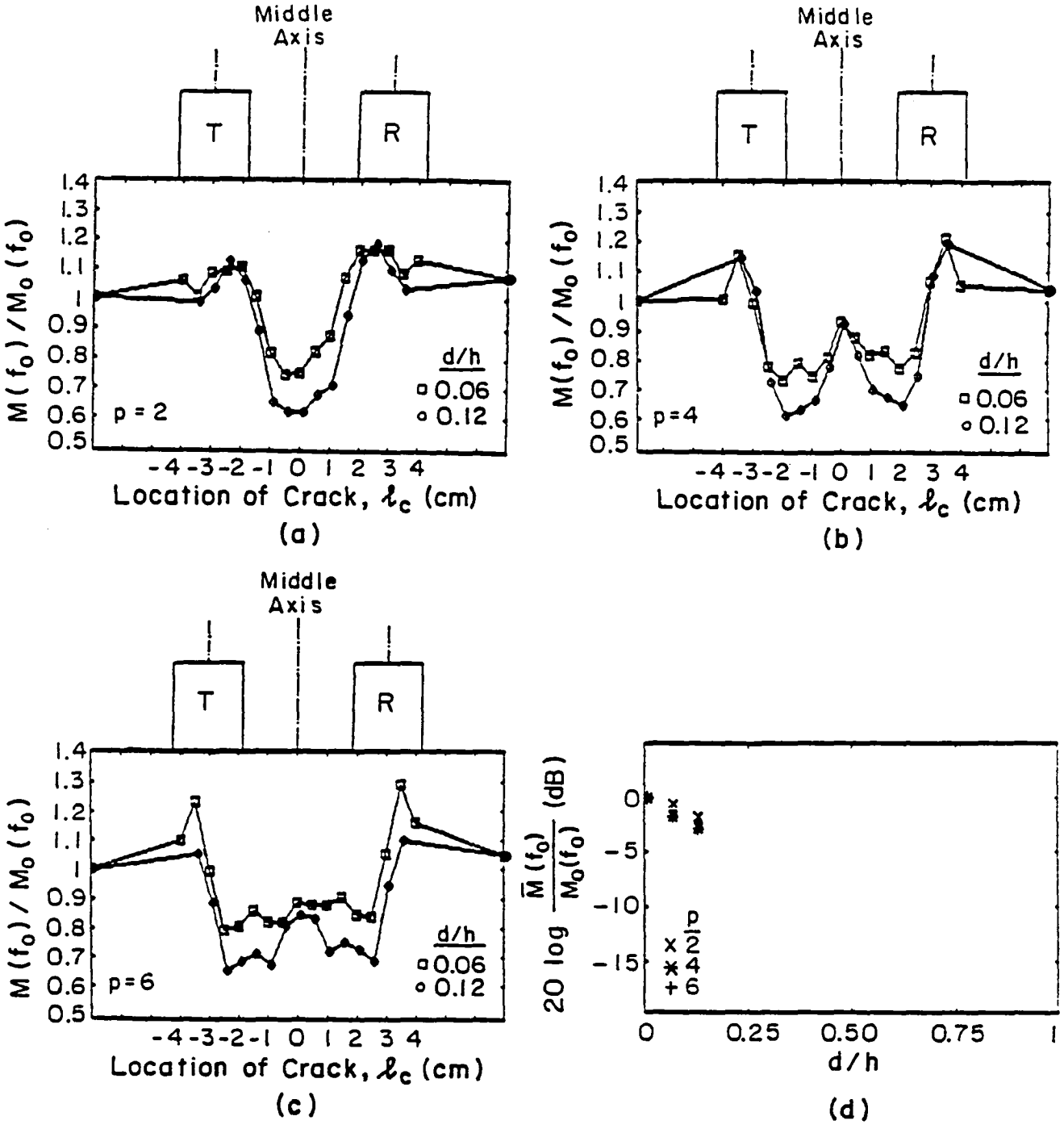

Fig. 10 $M(f_o)/M_o(f_o)$ for reflections with (a) p=2, (b) p=4, and (c) p=6 versus ℓ_c for different d; and (d) 20 Log$[M(f_o)/M_o(f_o)]$ versus d/h for different p in specimens with h=10 cm (C0, C1, and C2).

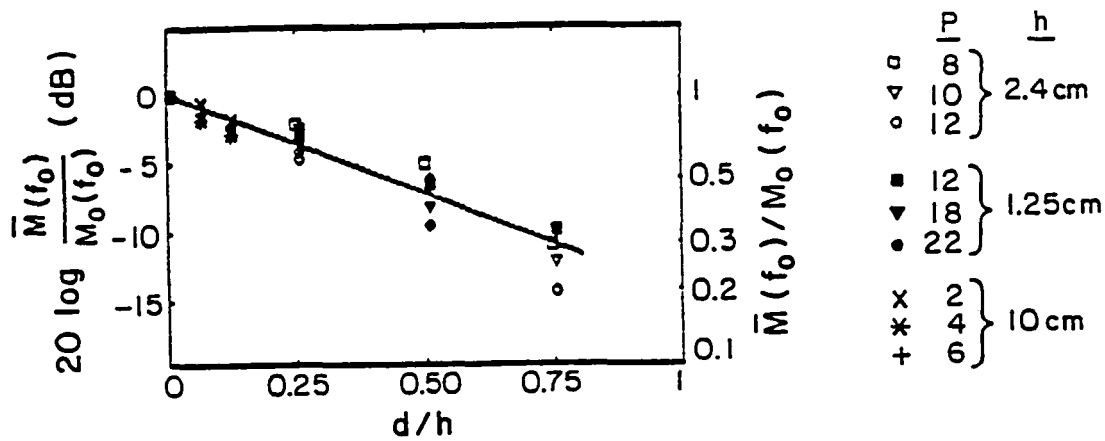

Fig. 11 Superposition of the data in Figs. 7 (d), 9 (d), and 10 (d) and the line fitted to superposed data by using least-squares criterion.

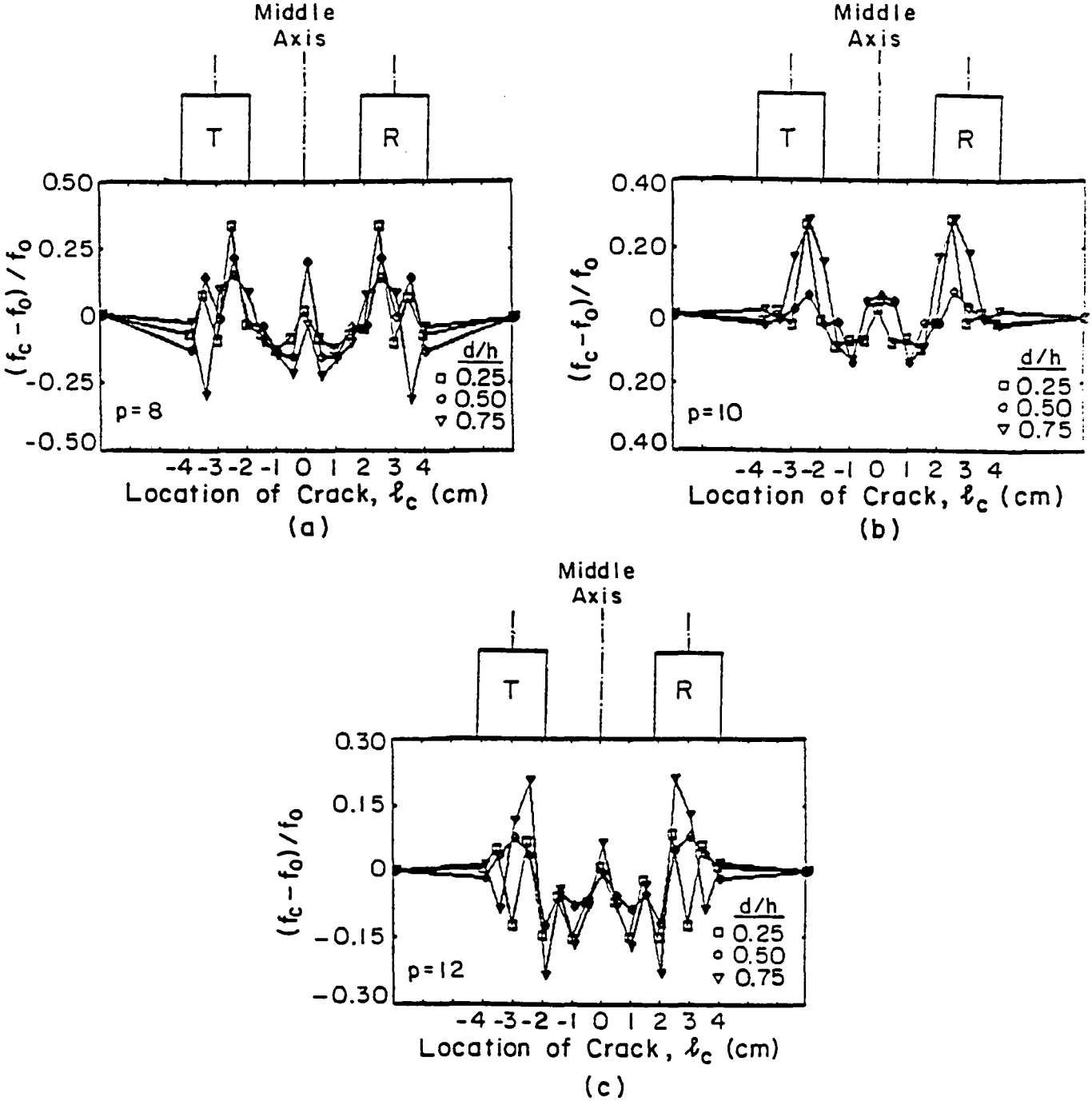

Fig. 12 $(f_c-f_o)/f_o$ for reflections with (a) p=8, (b) p=10, and (c) p=12 versus ℓ_c for different d in specimens with h=2.4 cm (A0, A1, A2, and A3).

1. Report No.	2. Government Accession No.	3. Recipient's Catalog No.
NASA CR-3904		

4. Title and Subtitle	5. Report Date
Ultrasonic Testing of Plates Containing Edge Cracks	June 1985
	6. Performing Organization Code

7. Author(s)	8. Performing Organization Report No.
James H. Williams, Jr., Hira Karagulle, and Samson S. Lee	None
	10. Work Unit No.

9. Performing Organization Name and Address	11. Contract or Grant No.
Massachusetts Institute of Technology Department of Mechanical Engineering Cambridge, Massachusetts 02139	NAG3-328
	13. Type of Report and Period Covered
	Contractor Report

12. Sponsoring Agency Name and Address	14. Sponsoring Agency Code
National Aeronautics and Space Administration Washington, D.C. 20546	506-53-1A (E-2550)

15. Supplementary Notes

Final report. Project Manager, Alex Vary, Structures Division, NASA Lewis Research Center, Cleveland OH 44135.

16. Abstract

The stress wave factor (SWF) signal is utilized for the nondestructive evaluation of plates containing perpendicular edge cracks. The effects of the existence, lateral location and depth of the crack on the magnitude spectra of individual reflections in the SWF signal are studied. If the reflections in the SWF signal are not overlapped the short-time Fourier analysis is applied. If the reflections are overlapped the short-time homomorphic analysis (cepstrum analysis) is applied. The magnitude ratio $M(f)/M_0(f)$ where $M(f)$ and $M_0(f)$ are the magnitudes of the Fourier transform of a reflection with and without a crack, respectively, and f is the frequency, is considered to study the effect of the crack. Several reflections which have average resonant frequencies approximately at 0.9, 1.3, and 1.7 MHz are analyzed. It is observed that the magnitude ratios evaluated at average resonant frequencies decrease more with increasing d/h if the crack is located between the transducers, where h is plate thickness and d is crack depth. Moreover, for the plates, crack geometries, reflections, and frequencies considered, the average decibel drop depends mainly on the dimensionless parameter d/h and it is approximately -1 dB per 0.07 d/h. Changes in the average resonant frequencies of the magnitude spectra are also observed due to changes in the location of the crack. However, no simple correlation between the average resonant frequency and crack depth can be stated.

17. Key Words (Suggested by Author(s))	18. Distribution Statement
Ultrasonics; Nondestructive testing; Stress wave factor; Frequency spectrum analysis; Plates; Cracks	Unclassified - Unlimited STAR Category 38

19. Security Classif. (of this report)	20. Security Classif. (of this page)	21. No. of pages	22. Price
Unclassified	Unclassified	36	A03

For sale by the National Technical Information Service, Springfield, Virginia 22161 NASA-Langley, 1985

National Aeronautics and
Space Administration

Washington, D.C.
20546

Official Business
Penalty for Private Use, $300

THIRD-CLASS BULK RATE

BULK RATE
POSTAGE & FEES PAID
NASA Washington, DC
Permit No. G-27

POSTMASTER: If Undeliverable (Section 158 Postal Manual) Do Not Return